

Redox-Active Behavior of the $[\{\text{Ti}(\eta^5\text{-C}_5\text{Me}_5)(\mu\text{-NH})\}_3(\mu_3\text{-N})]$ Metalloligand

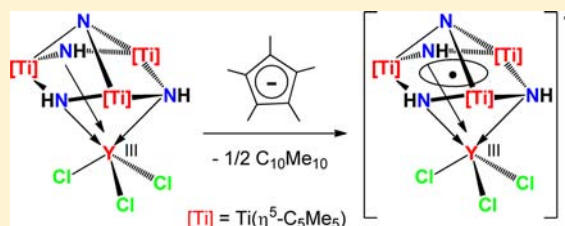
Jorge Caballo,[†] Jorge J. Carbó,[‡] Miguel Mena,[†] Adrián Pérez-Redondo,[†] Josep-M. Poble,[‡] and Carlos Yélamos^{*,†}

[†]Departamento de Química Inorgánica, Universidad de Alcalá, 28871 Alcalá de Henares-Madrid, Spain

[‡]Department de Química Física i Inorgánica, Universitat Rovira i Virgili, Marcel·lí Domingo s/n, 43007 Tarragona, Spain

Supporting Information

ABSTRACT: Treatment of $[\text{Cl}_3\text{Y}\{(\mu_3\text{-NH})_3\text{Ti}_3(\eta^5\text{-C}_5\text{Me}_5)_3(\mu_3\text{-N})\}]$ with $[\text{K}(\text{C}_5\text{Me}_5)]$ in toluene gives $\text{C}_{10}\text{Me}_{10}$ and the paramagnetic $[\text{K}(\mu\text{-Cl})_3\text{Y}\{(\mu_3\text{-NH})_3\text{Ti}_3(\eta^5\text{-C}_5\text{Me}_5)_3(\mu_3\text{-N})\}]$ (3) derivative. Crystallization of 3 in pyridine affords the potassium-free $[\text{Cl}_2(\text{py})_2\text{Y}\{(\mu_3\text{-NH})_3\text{Ti}_3(\eta^5\text{-C}_5\text{Me}_5)_3(\mu_3\text{-N})\}]$ (4) complex. Whereas the reaction of 3 with 1 equiv of 18-crown-6 leads to the molecular complex $[(18\text{-crown-6})\text{K}(\mu\text{-Cl})_3\text{Y}\{(\mu_3\text{-NH})_3\text{Ti}_3(\eta^5\text{-C}_5\text{Me}_5)_3(\mu_3\text{-N})\}]$ (5), the analogous treatment of 3 with cryptand-222 affords the ion pair $[\text{K}(\text{crypt-222})][\text{Cl}_3\text{Y}\{(\mu_3\text{-NH})_3\text{Ti}_3(\eta^5\text{-C}_5\text{Me}_5)_3(\mu_3\text{-N})\}]$ (6). The X-ray crystal structures of 4, 5, and 6 have been determined. Density functional theory (DFT) calculations have elucidated the electronic structure of these species, which should be regarded as containing trivalent Y bonded to the $\{(\mu_3\text{-NH})_3\text{Ti}_3(\eta^5\text{-C}_5\text{Me}_5)_3(\mu_3\text{-N})\}$ metalloligand radical anion.



INTRODUCTION

An emergent theme of contemporary research interest is the synthesis and reactivity of metal complexes bearing ligands with redox-active behavior.¹ Such species are relevant in the field of bioinorganic chemistry,² and offer interesting prospects to uncover new catalytic reactions.^{1b,3} In particular, the ability of redox-active ligands to function as “electron reservoirs” can be exploited for multiple-electron transformations in metal complexes that are reluctant to such transformations otherwise. For instance, several research groups have investigated electrophilic d⁰ early transition metals supported by redox-active ligands to promote redox reactions (e.g., nitrene transfer, oxidative addition, reductive elimination) which are unexpected because of the stability of high oxidation states of those metals.⁴ In those events, the metal maintains its most stable oxidation state while the ligand accepts or delivers the electron density associated with the chemical reaction.

Over the past decade we have been involved in the study of the reactivity of the trimetallic imido-nitrido titanium(IV) derivative $[\{\text{Ti}(\eta^5\text{-C}_5\text{Me}_5)(\mu\text{-NH})\}_3(\mu_3\text{-N})]$ (1). Complex 1 is capable of acting as a Lewis base through the imido groups toward many metal derivatives to give cube-type adducts $[\text{L}_n\text{M}\{(\mu_3\text{-NH})_3\text{Ti}_3(\eta^5\text{-C}_5\text{Me}_5)_3(\mu_3\text{-N})\}]$.⁶ In particular, we have recently demonstrated the ability of 1 to act as a rigid tridentate chelate metalloligand toward group 3 and lanthanide metal halides.⁷ Subsequent treatment of the yttrium complex $[\text{Cl}_3\text{Y}\{(\mu_3\text{-NH})_3\text{Ti}_3(\eta^5\text{-C}_5\text{Me}_5)_3(\mu_3\text{-N})\}]$ (2) with sodium cyclopentadienide (1 equiv) in toluene gave an orange solution from which the expected derivative $[\text{CpCl}_2\text{Y}\{(\mu_3\text{-NH})_3\text{Ti}_3(\eta^5\text{-C}_5\text{Me}_5)_3(\mu_3\text{-N})\}]$ was isolated as a diamagnetic orange solid.^{7a} In contrast, we report here on the analogous reaction of 2 with

potassium pentamethylcyclopentadienide to afford the immediate precipitation of $[\text{K}(\mu\text{-Cl})_3\text{Y}\{(\mu_3\text{-NH})_3\text{Ti}_3(\eta^5\text{-C}_5\text{Me}_5)_3(\mu_3\text{-N})\}]$ (3) as a paramagnetic green solid. A combination of experimental and theoretical studies on this novel compound and derivatives thereof has shown that complex 1 behaves as a redox-active metalloligand.

EXPERIMENTAL SECTION

General Considerations. All manipulations were carried out under argon atmosphere using Schlenk flask line or glovebox techniques. Toluene and hexane were distilled from Na/K alloy just before use. Pyridine was distilled from calcium hydride just prior to use. NMR solvents were dried with Na/K alloy (C_6D_6) or calcium hydride (CDCl_3 , $\text{C}_5\text{D}_5\text{N}$) and vacuum-distilled. Oven-dried glassware was repeatedly evacuated with a pumping system (ca. 1×10^{-3} Torr) and subsequently filled with inert gas. 1,4,7,10,13,16-Hexaoxacyclooctadecane (18-crown-6) was purchased from Aldrich and used as received. 4,7,13,16,21,24-Hexaoxa-1,10-diazabicyclo[8.8.8]hexacoxane (crypt-222) was purchased from Acros and used as received. $[\text{Cl}_3\text{Y}\{(\mu_3\text{-NH})_3\text{Ti}_3(\eta^5\text{-C}_5\text{Me}_5)_3(\mu_3\text{-N})\}]$ ⁷ (2) and $[\text{K}(\text{C}_5\text{Me}_5)]$ ⁸ were prepared according to published procedures.

Samples for infrared spectroscopy were prepared as KBr pellets, and the spectra were obtained using an FT-IR Perkin-Elmer SPECTRUM 2000 spectrophotometer. ¹H NMR spectra were recorded on a Varian Unity-300 spectrometer. Chemical shifts (δ , ppm) in the ¹H NMR spectra are given relative to residual protons of the solvent. The effective magnetic moments were determined by the Evans NMR method at 293 K (using a 300 MHz instrument with a field strength of 7.05 T).⁹ Microanalyses (C, H, N) were performed in a Leco CHNS-932 microanalyzer.

Received: February 21, 2013

Published: May 1, 2013



Table 1. Experimental Data for the X-ray Diffraction Studies on Complexes 4, 5, and 6

	4-C ₅ H ₅ N	5-7C ₆ D ₆	6-C ₆ D ₆
formula	C ₄₅ H ₆₃ Cl ₂ N ₇ Ti ₃ Y	C ₈₄ H ₁₁₄ Cl ₃ KN ₄ O ₆ Ti ₃ Y	C ₅₄ H ₉₀ Cl ₃ KN ₆ O ₆ Ti ₃ Y
M _r	1005.53	1653.85	1297.38
T [K]	200(2)	200(2)	200(2)
λ [Å]	0.71073	0.71073	0.71073
crystal system	monoclinic	trigonal	triclinic
space group	P2 ₁ /c	P $\bar{3}$	P $\bar{1}$
a [Å]; α [deg]	17.574(10)	16.527(4)	11.046(1); 82.44(2)
b [Å]; β [deg]	12.113(5); 94.58(3)	16.527(3)	11.857(2); 77.73(2)
c [Å]; γ [deg]	22.576(15)	18.067(4)	25.280(8); 89.48(1)
V [Å ³]	4790(5)	4274(2)	3207(1)
Z	4	2	2
ρ _{calcd} [g cm ⁻³]	1.394	1.285	1.344
μ _{MoKα} [mm ⁻¹]	1.831	1.136	1.494
F(000)	2084	1738	1358
crystal size [mm ³]	0.36 × 0.24 × 0.20	0.20 × 0.20 × 0.20	0.51 × 0.18 × 0.15
θ range (deg)	3.06 to 27.51°	3.06 to 27.51°	3.13 to 27.50°
index ranges	-22 to 22, -15 to 15, 0 to 29	-21 to 21, -21 to 21, 0 to 23	-14 to 14, -15 to 15, -32 to 32
reflections collected	100604	58887	75805
unique data	10986 [R(int) = 0.065]	6547 [R(int) = 0.111]	14695 [R(int) = 0.137]
obsd data [I > 2σ(I)]	7610	4243	7653
goodness-of-fit on F ²	1.073	1.069	1.073
final R ^a indices [I > 2σ(I)]	R1 = 0.046, wR2 = 0.107	R1 = 0.082, wR2 = 0.223	R1 = 0.078, wR2 = 0.173
R ^a indices (all data)	R1 = 0.083, wR2 = 0.118	R1 = 0.117, wR2 = 0.239	R1 = 0.172, wR2 = 0.213
largest diff. peak/hole [e Å ⁻³]	0.616 and -0.831	0.790 and -0.626	0.849 and -1.408

$$^a R1 = \frac{\sum |F_o| - |F_c|}{\sum |F_o|}, wR2 = \left\{ \frac{\sum w(F_o^2 - F_c^2)^2}{\sum w(F_o^2)^2} \right\}^{1/2}.$$

Synthesis of [K(μ-Cl)₃Y(μ₃-NH)₃Ti₃(η⁵-C₅Me₅)₃(μ₃-N)] (3). A 100 mL amber stained Schlenk flask was charged with 2 (0.50 g, 0.62 mmol), [K(C₅Me₅)] (0.11 g, 0.62 mmol), and toluene (20 mL). The reaction mixture was stirred at room temperature for 24 h to give an abundant green solid and a green solution. The solid was isolated by filtration onto a glass frit and vacuum-dried to afford 3 as a dark green powder (0.37 g, 71%). IR (KBr, cm⁻¹): $\tilde{\nu}$ 3333 (s), 2971 (s), 2906 (vs), 2857 (vs), 2724 (w), 1494 (m), 1431 (s), 1377 (vs), 1238 (w), 1067 (w), 1026 (m), 914 (w), 772 (m), 729 (s), 695 (m), 657 (vs), 511 (w), 441 (w). ¹H NMR (300 MHz, C₆D₆, 20 °C): δ 10.9 (s br., Δν_{1/2} = 151 Hz; C₅Me₅). Anal. Calcd (%) for C₃₀H₄₈Cl₃KN₄Ti₃Y (M_w = 842.69): C 42.76, H 5.74, N 6.65. Found: C 43.45, H 5.82, N 6.53. The effective magnetic moment of 3 was determined to be 1.60 μ_B (based on a unit formula of C₃₀H₄₈Cl₃KN₄Ti₃Y) on a C₆D₆ solution.

Synthesis of [Cl₂(py)₂Y(μ₃-NH)₃Ti₃(η⁵-C₅Me₅)₃(μ₃-N)] (4). A 100 mL Schlenk flask was charged with 3 (0.40 g, 0.48 mmol) and pyridine (10 mL). The resultant dark green solution was concentrated under vacuum to the half of the volume and filtered. After cooling at -30 °C for 2 days, dark green crystals of 4·C₅H₅N suitable for a single crystal X-ray diffraction determination were grown. The crystals were dried under dynamic vacuum for 8 h and characterized as 4 (0.13 g, 30%). IR (KBr, cm⁻¹): $\tilde{\nu}$ 3336 (m), 2970 (m), 2905 (vs), 2856 (s), 2723 (w), 1599 (m), 1487 (m), 1441 (vs), 1376 (vs), 1222 (w), 1152 (w), 1068 (w), 1038 (m), 1026 (m), 1002 (w), 801 (w), 760 (s), 705 (vs), 667 (vs), 623 (vs), 512 (m), 429 (m). ¹H NMR (300 MHz, C₅D₅N, 20 °C): δ 10.2 (s br., Δν_{1/2} = 33 Hz; C₅Me₅). Anal. Calcd (%) for C₄₀H₅₈Cl₂N₆Ti₃Y (M_w = 926.35): C 51.86, H 6.31, N 9.07. Found: C 52.61, H 6.40, N 9.66. The effective magnetic moment of 4 was determined to be 1.88 μ_B (based on a unit formula of C₄₀H₅₈Cl₂N₆Ti₃Y) on a C₅D₅N solution.

Synthesis of [(18-crown-6)K(μ-Cl)₃Y(μ₃-NH)₃Ti₃(η⁵-C₅Me₅)₃(μ₃-N)] (5). A 100 mL ampule (Teflon stopcock) was charged with 3 (0.30 g, 0.36 mmol), 18-crown-6 (0.094 g, 0.36 mmol), and toluene (40 mL). The reaction mixture was stirred at 80 °C for 2 days to give a green solution and a fine green solid. The solid was eliminated by filtration, and the volatile components of the solution were removed under reduced pressure to afford 5 as a green solid (0.25 g, 63%). IR (KBr, cm⁻¹): $\tilde{\nu}$ 3334 (w), 2903 (s), 1452 (m), 1376

(m), 1351 (s), 1284 (w), 1251 (m), 1111 (vs), 1027 (w), 964 (m), 840 (w), 791 (w), 718 (s), 659 (s), 520 (w), 422 (w). ¹H NMR (300 MHz, C₆D₆, 20 °C): δ 10.8 (s br., Δν_{1/2} = 5 Hz; C₅Me₅), 3.4 (s br., Δν_{1/2} = 6 Hz; OCH₂CH₂O). Anal. Calcd (%) for C₄₂H₇₂Cl₃KN₄O₆Ti₃Y (M_w = 1107.02): C 45.57, H 6.56, N 5.06. Found: C 45.36, H 6.78, N 5.44. The effective magnetic moment of 5 was determined to be 1.76 μ_B (based on a unit formula of C₄₂H₇₂Cl₃KN₄O₆Ti₃Y) on a C₆D₆ solution.

Synthesis of [K(crypt-222)]Cl₃Y(μ₃-NH)₃Ti₃(η⁵-C₅Me₅)₃(μ₃-N)] (6). A 100 mL Schlenk flask was charged with 3 (0.20 g, 0.24 mmol), crypt-222 (0.089 g, 0.24 mmol), and toluene (20 mL). The reaction mixture was stirred at ambient temperature for 24 h to give a green solid and a green solution. The solid was isolated by filtration onto a glass frit and vacuum-dried to afford 6 as a green powder (0.17 g, 59%). IR (KBr, cm⁻¹): $\tilde{\nu}$ 3327 (w), 2895 (s), 2816 (m), 1477 (w), 1448 (m), 1375 (w), 1354 (m), 1299 (w), 1261 (w), 1132 (s), 1099 (vs), 1028 (w), 951 (m), 931 (w), 830 (w), 752 (w), 638 (w), 523 (w), 420 (w). ¹H NMR (300 MHz, C₅D₅N, 20 °C): δ 11.1 (s br., Δν_{1/2} = 33 Hz; C₅Me₅), 3.40 (s, 12H; OCH₂CH₂O), 3.34 (t, ³J(H,H) = 4.5 Hz, 12H; OCH₂CH₂N), 2.34 (t, ³J(H,H) = 4.5 Hz, 12H; OCH₂CH₂N). Anal. Calcd (%) for C₄₈H₈₄Cl₃KN₆O₆Ti₃Y (M_w = 1219.19): C 47.29, H 6.94, N 6.89. Found: C 47.44, H 7.01, N 6.47. The effective magnetic moment of 6 was determined to be 1.94 μ_B (based on a unit formula of C₄₈H₈₄Cl₃KN₆O₆Ti₃Y) on a C₅D₅N solution.

X-ray Structure Determination of 4, 5, and 6. Green crystals of 4·C₅H₅N were grown in pyridine at -30 °C as described in the Experimental Section. Green crystals of 5·7C₆D₆ and 6·C₆D₆ were obtained by slow cooling at room temperature of benzene-d₆ solutions of the compounds heated at 80 °C in NMR tubes. The crystals were removed from the Schlenk flask or NMR tube and covered with a layer of a viscous perfluoropolyether (FomblinY). A suitable crystal was selected with the aid of a microscope, mounted on a cryoloop, and immediately placed in the low temperature nitrogen stream of the diffractometer. The intensity data sets were collected at 200 K on a Bruker-Nonius KappaCCD diffractometer equipped with an Oxford Cryostream 700 unit. Crystallographic data for all the complexes are presented in Table 1.

The structures were solved, using the WINGX package,¹⁰ by direct (4 and 6) or Patterson (5) methods (SHELXS-97)¹¹ and refined by least-squares against F^2 (SHELXL-97).¹¹ Compound 4 crystallized with a molecule of pyridine, which presented disorder. This disorder was treated by using the PART tool, allowing free refinement of the occupancy factors with the FVAR command of the SHELXL-97 program. The final values for the occupancy factors were 65 and 35% for each position. Furthermore the geometry of this solvent molecule was constrained to be a regular hexagon. All non-hydrogen atoms were anisotropically refined, except those that formed the disordered molecule of pyridine [C(91), C(92), C(93), C(94), C(95), N(10), C(91)', C(92)', C(93)', C(94)', C(95)' and N(10)'], which were refined isotropically. The hydrogen atoms were positioned geometrically and refined by using a riding model in the last cycles of refinement.

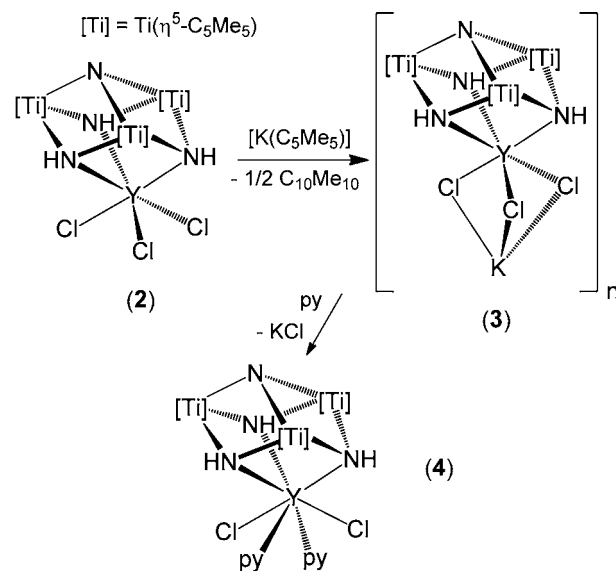
Compound 5 crystallized with seven molecules of benzene, which were found in the difference Fourier map, but it was not possible to obtain a chemically sensible model for them, so the Squeeze¹² procedure was used to remove their contribution to the structure factors. By contrast, 6 crystallized with a benzene molecule, which was constrained to be a regular hexagon. In the crystallographic study of both complexes 5 and 6, all non-hydrogen atoms were refined anisotropically, whereas all hydrogen atoms were included, positioned geometrically, and refined by using a riding model.

Computational Details. All DFT calculations were carried out with the ADF program¹³ by using triple- ζ and polarization Slater basis sets to describe the valence electrons of C, N, Cl, and Y. For titanium, a frozen core composed of the 1s, 2s, and 2p orbitals was described by double- ζ Slater functions, the 3d and 4s orbitals by triple- ζ functions, and the 4p orbital by a single orbital. Hydrogen atoms were described by triple- ζ and polarization functions. The geometries and binding energies were calculated with gradient corrections. We used the local spin density approximation, characterized by the electron gas exchange ($X\alpha$ with $\alpha = 2/3$) together with Vosko–Wilk–Nusair parametrization¹⁴ for correlation. Becke's nonlocal corrections¹⁵ to the exchange energy and Perdew's nonlocal corrections¹⁶ to the correlation energy were added. Quasirelativistic corrections were employed by using the ZORA formalism with corrected core potentials. The quasirelativistic frozen core shells were generated with the auxiliary program DIRAC. COSMO approach was used to incorporate solvent effects in the calculations,¹⁷ which are relevant in case of anionic structures.¹⁸

RESULTS AND DISCUSSION

The reaction of 2 with 1 equiv of $[K(C_5Me_5)]$ in benzene- d_6 at room temperature was monitored by NMR spectroscopy (Scheme 1). Immediately, the initial yellow suspension turned to a green color and an abundant green solid was deposited at the bottom of the NMR tube. Analysis of the supernatant green solution by 1H NMR spectroscopy only showed resonance signals assigned to $C_{10}Me_{10}$ along with a minor broad resonance at $\delta = 10.9$. The analogous treatment of 2 with 1 equiv of $[K(C_5Me_5)]$ in toluene at room temperature was carried out in the absence of light to give complex $[K(\mu-Cl)_3Y\{(\mu_3-NH)_3Ti_3(\eta^5-C_5Me_5)_3(\mu_3-N)\}]$ (3) as a dark green solid in 71% yield. Compound 3 exhibits a poor solubility in hydrocarbon solvents, but its 1H NMR spectrum in benzene- d_6 only shows the far-downfield and very broad resonance ($\delta = 10.9$, $\Delta\nu_{1/2} = 151$ Hz) mentioned above for the C_5Me_5 protons. The paramagnetic nature of 3 was confirmed by an Evans method determination of its magnetic susceptibility ($\mu_{eff} = 1.60 \mu_B$, 293 K, C_6D_6 solution),⁹ which indicated the presence of an unpaired electron in the complex. This result, along with the exclusive formation of $C_{10}Me_{10}$ as byproduct, which most likely is formed via coupling of pentamethylcyclopentadienyl radicals,¹⁹ suggests that the reaction pathway for the synthesis of 3 consists in an electron transfer from the $C_5Me_5^-$ anion to

Scheme 1. Reaction of 2 with $[K(C_5Me_5)]$



the yttrium/titanium cube-type complex 2. The resultant reduced specie retains one potassium cation as part of the structure according to analytical data and reactivity studies (see below).

Whereas the presence of ambient light in the synthesis of 3 afforded a less pure bulk material with concomitant lower yield of the product, once isolated in the solid-state or in benzene- d_6 solution, compound 3 is stable under normal fluorescent laboratory light. However, complex 3 exhibits a high air-sensitivity and immediately reacts with chloroform- d_1 to regenerate 2. Compound 3 readily dissolves in pyridine to give a green solution which upon cooling at -30 °C afforded dark green crystals of the adduct $[Cl_2(py)_2Y\{(\mu_3-NH)_3Ti_3(\eta^5-C_5Me_5)_3(\mu_3-N)\}]$ (4) suitable for analysis by a single crystal X-ray diffraction determination. Crystals of 4 bear one pyridine solvent molecule per cube-type unit, but these crystallization molecules are easily lost under dynamic vacuum according to IR spectroscopy and analytical data. The molecular structure of 4 shows an $[YTi_3N_4]$ cube-type core with the ligand $[(\mu_3-NH)_3Ti_3(\eta^5-C_5Me_5)_3(\mu_3-N)]$ coordinating in a tripodal fashion to yttrium (Figure 1 and Table 2). In addition, yttrium is bonded to two chloride and two pyridine ligands to give a seven-coordinate environment. The geometry about yttrium is best described as distorted capped trigonal prismatic with one tighter triangle defined by the three nitrogen atoms of the metalloligand, a more open one defined by the Cl(2), N(41), and N(51) atoms, and with the Cl(1) atom capping one rectangular face of the prism. This is clearly seen by comparing the N–Y–N angles within the cube (average $72.0(2)^\circ$) and the Cl(2)–Y–N(41) $78.3(1)^\circ$, Cl(2)–Y–N(51) $79.3(1)^\circ$, and N(41)–Y–N(51) $128.3(1)^\circ$ angles. The Y–N bond lengths with the metalloligand range between 2.416(3) and 2.508(3) Å, and compare well with those determined for the tris(pyrazolyl)borate ligand in the $[YCl_2\{HB(3,5-Me_2pz)_3\}(phen)]$ complex (average 2.448(6) Å).²⁰ The Y–Cl and Y–N(py) bond lengths in 4 of average 2.640(3) and 2.65(2) Å, respectively, are slightly longer than those found in the yttrium tris(pyrazolyl)borate derivative (average Y–Cl and Y–N(phen) are 2.600(2) and 2.544(6) Å, respectively)²⁰ and the adduct $[YCl_3(py)_2]$ (average Y–Cl and Y–N(py) are 2.61(2) and 2.55(3) Å).²¹ Within the titanium metalloligand, the distortions in bond

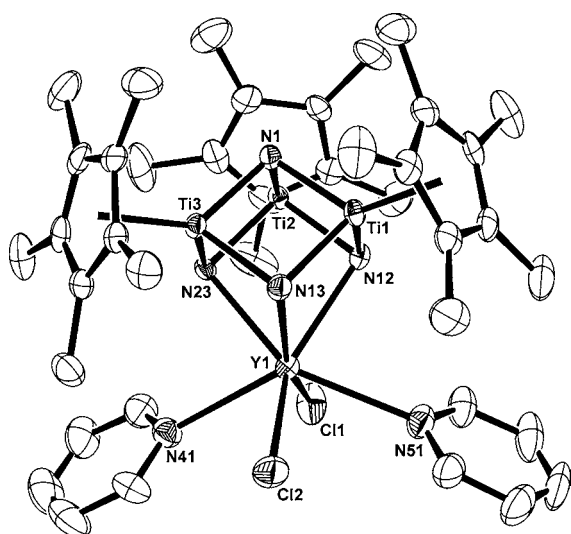


Figure 1. Perspective view of complex **4** with displacement ellipsoids at the 50% probability level. Hydrogen atoms and the pyridine solvent molecule are omitted for clarity.

Table 2. Selected Lengths (Å) and Angles (deg) for Complex **4**

Y(1)–N(12)	2.472(3)	Y(1)–N(13)	2.508(3)
Y(1)–N(23)	2.416(3)	Y(1)–Cl(1)	2.637(2)
Y(1)–Cl(2)	2.643(2)	Y(1)–N(41)	2.667(3)
Y(1)–N(51)	2.635(3)	Ti–N(1) av	1.91(2)
Ti–N av	1.98(1)	Ti(1)···Ti(2)	2.812(1)
Ti(1)···Ti(3)	2.826(1)	Ti(2)···Ti(3)	2.831(2)
Ti···Y(1) av	3.33(2)		
N(12)–Y(1)–N(13)	71.7(1)	N(12)–Y(1)–N(23)	72.1(1)
N(13)–Y(1)–N(23)	72.3(1)	Cl(1)–Y(1)–Cl(2)	120.8(1)
N(41)–Y(1)–N(51)	128.3(1)	Cl(1)–Y(1)–N(41)	75.9(1)
Cl(1)–Y(1)–N(51)	76.8(1)	Cl(2)–Y(1)–N(41)	78.3(1)
Cl(2)–Y(1)–N(51)	79.3(1)	N(12)–Y(1)–Cl(1)	90.0(1)
N(12)–Y(1)–Cl(2)	136.6(1)	N(12)–Y(1)–N(41)	143.0(1)
N(12)–Y(1)–N(51)	79.3(1)	N(13)–Y(1)–Cl(1)	161.3(1)
N(13)–Y(1)–Cl(2)	77.0(1)	N(13)–Y(1)–N(41)	116.3(1)
N(13)–Y(1)–N(51)	103.0(1)	N(23)–Y(1)–Cl(1)	98.6(1)
N(23)–Y(1)–Cl(2)	125.3(1)	N(23)–Y(1)–N(41)	76.4(1)
N(23)–Y(1)–N(51)	151.1(1)	N(1)–Ti–N av	87.0(9)
N–Ti–N av	94.2(5)	Ti–N(1)–Ti av	95(1)
Ti–N–Ti av	91.0(7)	Y(1)–N–Ti av	96.3(9)

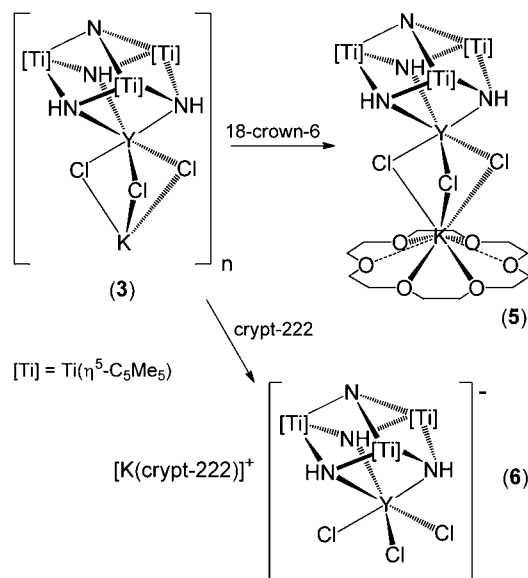
distances and angles in **4** are small when compared to those of **1**.^{5a}

The ¹H NMR spectrum of **4** in pyridine-d₅ shows one downfield and broad resonance ($\delta = 10.2$, $\Delta\nu_{1/2} = 33$ Hz) for the C₅Me₅ groups. That resonance and the magnetic susceptibility determined by the Evans method ($\mu_{\text{eff}} = 1.88 \mu_{\text{B}}$, 293 K, C₅D₅N solution) compare well with those found for **3**. A very similar resonance signal ($\delta = 10.5$, $\Delta\nu_{1/2} = 380$ Hz) has been recently reported for the paramagnetic [Ti(η^5 -C₅Me₅)Cl₃][−] titanate anion in a dichloromethane-d₂ solution.²²

While compound **4** adopts a molecular structure that consists of isolated cube-type units, complex **3** retains a potassium atom per cube-type core and presumably has a polymeric structure. Despite many attempts we failed to grow suitable crystals of **3** for an X-ray crystal structure determination. To gain insight into the structure of **3**, we studied its reaction with macrocyclic

polyethers which are prone to coordinate potassium ions (Scheme 2). Treatment of compound **3** with 1 equiv of 18-

Scheme 2. Reactions of **3** with Macrocyclic Polyethers



crown-6 in toluene at 80 °C gave a green solution from which the molecular complex [(18-crown-6)K(μ -Cl)₃Y{(μ_3 -NH)₃Ti₃(η^5 -C₅Me₅)₃(μ_3 -N)}] (**5**) was isolated in 63% yield as a green solid. In contrast, the reaction of **3** with cryptand-222 gave the immediate precipitation of the ionic complex [K(crypt-222)][Cl₃Y{(μ_3 -NH)₃Ti₃(η^5 -C₅Me₅)₃(μ_3 -N)}] (**6**) as a green powder in 59% yield. Whereas compound **5** exhibits an enhanced solubility in benzene and toluene when compared with **3**, complex **6** is poorly soluble in those solvents but exhibits a good solubility in pyridine. Both compounds immediately react with chloroform-d₁ to give yellow solutions of complex **2** and the corresponding free macrocyclic polyether according to NMR spectroscopy.

The ¹H NMR spectrum of **5** in benzene-d₆ shows two broad resonances at $\delta = 10.8$ ($\Delta\nu_{1/2} = 5$ Hz) and $\delta = 3.4$ ($\Delta\nu_{1/2} = 6$ Hz) attributed to the C₅Me₅ and the crown ether ligands, respectively. Similarly, the ¹H NMR spectrum of **6** in pyridine-d₅ reveals one broad resonance at $\delta = 11.1$ ($\Delta\nu_{1/2} = 33$ Hz) for the C₅Me₅ groups and three well-defined resonances at $\delta = 3.40$ (s), 3.34 (t, ³J(H,H) = 4.5 Hz), and 2.34 (t, ³J(H,H) = 4.5 Hz) for the methylene groups of the cryptand-222 ligand. The magnetic moment measurements by the Evans method gave $\mu_{\text{eff}} = 1.76 \mu_{\text{B}}$ for **5** and $\mu_{\text{eff}} = 1.94 \mu_{\text{B}}$ for **6** confirming their paramagnetic nature with an unpaired electron.

Crystals of **5**·7C₆D₆ were grown by slow cooling at room temperature of a benzene-d₆ solution heated at 80 °C. The molecular structure shows an [YTi₃N₄] cube-type core connected to one potassium atom by three bridging chloride ligands (Figure 2 and Table 3). Molecules of **5** present a C₃ axis which crosses the N(1), Y(1), and K(1) atoms. The yttrium atom exhibits a distorted trigonal antiprismatic geometry with one tighter triangle defined by the nitrogen atoms and with a more open one defined by the chloride ligands. The metalloligand coordinates to yttrium in a tridentate fashion with a Y(1)–N(11) bond length of 2.456(4) Å which is in the middle of the range of yttrium–nitrogen distances found in complex **4** (from 2.416(3) to 2.508(3) Å). The K(1)–Cl(1)

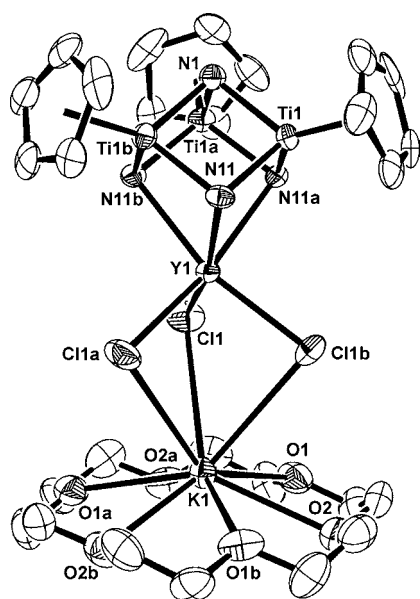


Figure 2. Simplified view of complex **5** with displacement ellipsoids at the 50% probability level. Methyl groups of the pentamethylcyclopentadienyl ligands and hydrogen atoms are omitted for clarity. Symmetry operation: (a) $1 - y, 1 + x - y, z$; (b) $-x + y, 1 - x, z$.

Table 3. Selected Lengths (Å) and Angles (deg) for Complex **5**^a

Y(1)–N(11)	2.456(4)	Y(1)–Cl(1)	2.585(1)
K(1)–Cl(1)	3.523(2)	K(1)–O(1)	2.870(4)
K(1)–O(2)	2.960(4)	Ti(1)–N(11)	1.937(4)
Ti(1)–N(1)	1.931(4)	Ti...Ti	2.792(2)
Y(1)...Ti	3.260(1)		
N(11)–Y(1)–N(11)a	72.3(1)	Cl(1)–Y(1)–Cl(1)a	93.3(1)
N(11)–Y(1)–Cl(1)	165.3(1)	N(11)–Y(1)–Cl(1)a	94.0(1)
N(11)–Y(1)–Cl(1)b	99.0(1)	Cl(1)–K(1)–Cl(1)a	64.5(1)
O(1)–K(1)–O(1)a	115.1(1)	O(1)–K(1)–O(2)	57.3(1)
O(1)–K(1)–O(2)a	58.1(1)	O(1)–K(1)–O(2)b	146.9(1)
O(2)–K(1)–O(2)a	108.7(1)	Cl(1)–K(1)–O(1)	80.8(1)
Cl(1)–K(1)–O(2)	121.5(1)	Cl(1)–K(1)–O(1)a	85.0(1)
Cl(1)–K(1)–O(2)a	72.3(1)	Cl(1)–K(1)–O(1)b	140.8(1)
Cl(1)–K(1)–O(2)b	126.8(1)	N(11)–Ti(1)–N(11)a	96.5(2)
N(1)–Ti(1)–N(11)	87.6(2)	N(1)–Ti(1)–N(11)a	87.8(2)
Y(1)–Cl(1)–K(1)	84.9(1)	Y(1)–N(11)–Ti(1)	94.8(1)
Y(1)–N(11)–Ti(1)b	95.1(2)	Ti(1)–N(11)–Ti(1)a	91.9(2)
Ti(1)–N(1)–Ti(1)a	92.6(2)		

^aSymmetry operation: (a) $1 - y, 1 + x - y, z$; (b) $-x + y, 1 - x, z$.

bond length of 3.523(2) Å indicates a weak interaction, but it is only slightly longer than those reported for complexes [(18-crown-6)K(μ -Cl)₃Pt(C₄Me₄)]²³ and [(18-crown-6)K(μ -Cl)₃Se]²⁴ (range 3.097–3.482 Å). As observed in those examples, a further indication of this K–Cl interaction is that the potassium atom is 0.83 Å above the plane defined by the six oxygen atoms of the 18-crown-6 ligand.

In contrast to **5** compound **6** crystallized from a benzene-d₆ solution as a well-separated ion pair, with the potassium cation encapsulated by the cryptand-222 ligand and the anion [Cl₃Y{(μ -NH)₃Ti₃(η^5 -C₅Me₅)₃(μ -N)}][−] showing a cube-type core (Figure 3 and Table 4). Crystals of **6** contain one benzene solvent molecule per ion pair. The yttrium atom exhibits a distorted trigonal antiprismatic geometry similar to

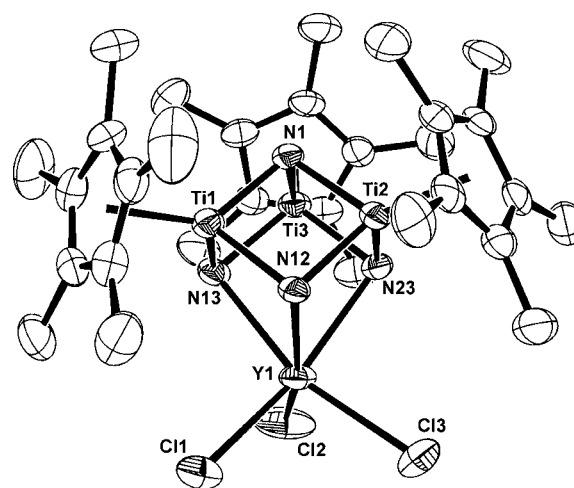


Figure 3. Perspective view of the anionic fragment of complex **6** with displacement ellipsoids at the 50% probability level. Hydrogen atoms are omitted for clarity.

that of **5**. Furthermore, the Y(1)–N and Y(1)–Cl bond lengths (average 2.475(9) and 2.595(9) Å, respectively) are very similar to those found in complex **5** (2.456(4) and 2.585(1) Å, respectively), confirming once again the weak coordination of the chloride bridging ligands to the potassium atom in **5**.

DFT calculations were conducted to establish the electronic structure of the paramagnetic complex **6**, and to gauge structural variation upon reduction (**2** vs **6**). The analysis of the electronic structure of [Cl₃Y{(μ -NH)₃Ti₃(η^5 -C₅Me₅)₃(μ -N)}][−] indicates that the additional electron is entirely delocalized among the three titanium atoms of the metal-ligand (electron spin density on Ti₃ core is ≈ 1.15 e, whereas on the Y atom is only ≈ 0.01 e). A two-electron reduction of the Ti₃ core has been previously observed in the reaction of terminal alkynes with titanium–zinc derivatives [(RCC)Zn]{(μ -N)(μ -NH)₂Ti₃(η^5 -C₅Me₅)₃(μ -N)}].²⁵ Figure 4 shows that the spin density of **6** is delocalized over the three Ti atoms. Its shape is consistent with the formal configuration with a single occupied titanium d orbital of *e* symmetry. Note that the lowest unoccupied molecular orbital (LUMO) of neutral [(Ti(η^5 -C₅Me₅)(μ -NH))₃(μ -N)] ligand was characterized as a combination of titanium d orbitals of *e*-type symmetry.²⁶ Because the extra electron resides in a formal *e* orbital, there is a first-order Jahn–Teller distortion that is manifested in Ti...Ti distances in both theoretical and experimental structures (Table 5). The same electronic structure has been observed for compound **4**, which exhibits an electron spin density localized on the Ti₃ core of ≈ 1.16 e.

The trend in computed distances on going from [Cl₃Y{(μ -NH)₃Ti₃(η^5 -C₅Me₅)₃(μ -N)}] (**2**) to the corresponding anion of **6** agrees rather well with the X-ray values (see Table 5).²⁷ It is worth mentioning that both computed and X-ray values suggest that the reduction is accompanied by a shortening of the Y–N bond distances and a subsequent lengthening of the Y–Cl bonds. This behavior is easy to rationalize from electrostatic arguments. The addition of an electron to an orbital centered in the Ti atoms favors the global electrostatic interaction between the trimetallic ligand and the Y³⁺ ion, shortening the Y–N bonding distances. The literature shows that stability of complexes with radical anion ligands is higher because of increased σ donor ability,²⁸ which can be also understood in terms of electrostatic interaction.

Table 4. Selected Lengths (Å) and Angles (deg) for Complex 6

Y(1)–N(12)	2.467(4)	Y(1)–N(13)	2.470(4)
Y(1)–N(23)	2.488(4)	Y(1)–Cl(1)	2.607(2)
Y(1)–Cl(2)	2.585(2)	Y(1)–Cl(3)	2.594(2)
Ti–N(1) av	1.93(1)	Ti–N av	1.98(1)
Ti...Ti av	2.84(2)	Y(1)...Ti av	3.32(1)
K(1)–N av	3.00(1)	K(1)–O	2.781(4)–2.885(4)
N(12)–Y(1)–N(13)	72.5(1)	N(12)–Y(1)–N(23)	71.9(1)
N(13)–Y(1)–N(23)	72.4(1)	Cl(1)–Y(1)–Cl(2)	99.2(1)
Cl(1)–Y(1)–Cl(3)	94.1(1)	Cl(2)–Y(1)–Cl(3)	97.4(1)
N(12)–Y(1)–Cl(1)	89.0(1)	N(12)–Y(1)–Cl(2)	162.1(1)
N(12)–Y(1)–Cl(3)	97.9(1)	N(13)–Y(1)–Cl(1)	100.3(1)
N(13)–Y(1)–Cl(2)	90.4(1)	N(13)–Y(1)–Cl(3)	162.4(1)
N(23)–Y(1)–Cl(1)	160.8(1)	N(23)–Y(1)–Cl(2)	98.6(1)
N(23)–Y(1)–Cl(3)	90.7(1)	N(1)–Ti–N av	87(1)
N–Ti–N av	95.0(1)	Ti–N(1)–Ti av	95(1)
Ti–N–Ti av	91.6(5)	Y(1)–N–Ti av	95.7(3)
O–K(1)–O	59.5(1)–142.0(1)	O–K(1)–N	59.5(1)–120.4(1)
N(2)–K(1)–N(3)	179.1(1)		

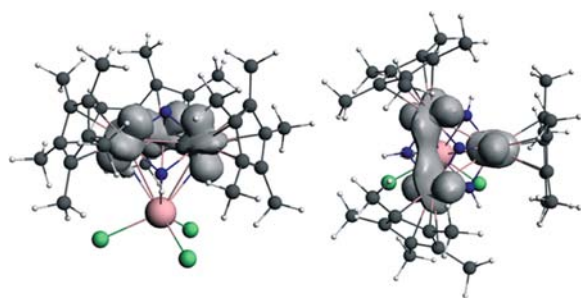


Figure 4. Representation of the electron spin density distribution computed for the $[\text{Cl}_3\text{Y}\{(\mu_3\text{-NH})_3\text{Ti}_3(\eta^5\text{-C}_5\text{Me}_5)_3(\mu_3\text{-N})\}]^-$ anion. Front view (left) and top view (right).

Table 5. Comparison of Selected Distances for $[\text{Cl}_3\text{Y}\{(\mu_3\text{-NH})_3\text{Ti}_3(\eta^5\text{-C}_5\text{Me}_5)_3(\mu_3\text{-N})\}]$ (2) and the Anion $[\text{Cl}_3\text{Y}\{(\mu_3\text{-NH})_3\text{Ti}_3(\eta^5\text{-C}_5\text{Me}_5)_3(\mu_3\text{-N})\}]^-$ of 6

	2		anion of 6	
	X-ray	DFT	X-ray	DFT
Y–N	2.573(7)	2.612	2.467(4)	2.483
	2.573(7)	2.615	2.470(4)	2.521
	2.589(7)	2.620	2.488(4)	2.529
Ti...Ti	2.851(2)	2.862	2.806(1)	2.840
	2.862(2)	2.864	2.852(2)	2.873
	2.869(2)	2.865	2.857(1)	2.887
Ti–NH	1.961(7)– 1.993(7)	1.971– 1.982	1.966(4)– 1.995(4)	1.988– 2.011
	Ti–N			
Ti–N	1.926(7)	1.942	1.914(4)	1.915
	1.926(7)	1.945	1.928(4)	1.945
	1.930(7)	1.945	1.945(4)	1.962
Y–Cl	2.540(3)	2.609	2.585(2)	2.674
	2.542(3)	2.610	2.594(2)	2.676
	2.576(3)	2.610	2.607(2)	2.676

CONCLUSION

We have demonstrated that $[\text{K}(\text{C}_5\text{Me}_5)]$ acts as an efficient one electron reductant to the yttrium complex $[\text{Cl}_3\text{Y}\{(\mu_3\text{-NH})_3\text{Ti}_3(\eta^5\text{-C}_5\text{Me}_5)_3(\mu_3\text{-N})\}]$ enabling the preparation of a series of paramagnetic tetrametallic cube-type derivatives. DFT calculations substantiate the assignment of the oxidation state

of the yttrium center in these species as trivalent with the $[(\mu_3\text{-NH})_3\text{Ti}_3(\eta^5\text{-C}_5\text{Me}_5)_3(\mu_3\text{-N})]$ metalloligand playing the role of electron density storage. The result opens perspectives for the use of $[\text{K}(\text{C}_5\text{Me}_5)]$ to generate a broad range of reduced polynuclear imido-nitrido complexes with interesting properties and chemical reactivity.

ASSOCIATED CONTENT

Supporting Information

X-ray crystallographic files in CIF format for complexes 4, 5, and 6. Cartesian coordinates for the computed structures of 2 and the anion of 6. This material is available free of charge via the Internet at <http://pubs.acs.org>.

AUTHOR INFORMATION

Corresponding Author

*Fax: (+34) 91-8854683. E-mail: carlos.yelamos@uah.es.

Notes

The authors declare no competing financial interest.

ACKNOWLEDGMENTS

We thank the Spanish MICINN (CTQ2008-00061/BQU and CTQ2011-0 29054-C02-01/BQU), Comunidad de Madrid and the Universidad de Alcalá (CCG10-UAH/PPQ-5935), Generalitat de Catalunya (2009SGR-00462 and XRTIC), and Factoría de Cristalización (CONSOLIDER-INGENIO 2010) for financial support of this research. J.C. thanks the MEC for a doctoral fellowship.

REFERENCES

- (a) Chirik, P. J. *Inorg. Chem.* **2011**, *50*, 9737–9740 and Forum Articles devoted to the topic in the *Inorg. Chem.* **2011** special issue 20. (b) de Bruin, B. *Eur. J. Inorg. Chem.* **2012**, 340–342 and articles devoted to the topic in the *Eur. J. Inorg. Chem.* **2012** special issue 3.
- (2) Kaim, W.; Schwederski, B. *Coord. Chem. Rev.* **2010**, *254*, 1580–1588.
- (3) (a) Allgeier, A. M.; Mirkin, C. A. *Angew. Chem., Int. Ed.* **1998**, *37*, 894–908. (b) Chirik, P. J.; Wieghardt, K. *Science* **2010**, *327*, 794–795. (c) Lyaskovskyy, V.; de Bruin, B. *ACS Catal.* **2012**, *2*, 270–279. (d) Praneeth, V. K. K.; Ringenberg, M. R.; Ward, T. R. *Angew. Chem., Int. Ed.* **2012**, *51*, 10228–10234 and references therein.

- (4) For selected recent articles in early transition metal chemistry, see: (a) Nguyen, A. L.; Zarkesh, R. A.; Lacy, D. C.; Thorson, M. K.; Heyduk, A. F. *Chem. Sci.* **2011**, *2*, 166–169. (b) Heyduk, A. F.; Zarkesh, R. A.; Nguyen, A. I. *Inorg. Chem.* **2011**, *50*, 9849–9863. (c) Tsurugi, H.; Saito, T.; Tanahashi, H.; Arnold, J.; Mashima, K. *J. Am. Chem. Soc.* **2011**, *133*, 18673–18683. (d) Lu, F.; Zarkesh, R. A.; Heyduk, A. F. *Eur. J. Inorg. Chem.* **2012**, 467–470. (e) Milsman, C.; Turner, Z. R.; Semproni, S. P.; Chirik, P. J. *Angew. Chem., Int. Ed.* **2012**, *51*, 5386–5390.
- (5) (a) Roesky, H. W.; Bai, Y.; Noltemeyer, M. *Angew. Chem., Int. Ed. Engl.* **1989**, *28*, 754–755. (b) Abarca, A.; Gómez-Sal, P.; Martín, A.; Mena, M.; Poblet, J.-M.; Yélamos, C. *Inorg. Chem.* **2000**, *39*, 642–651.
- (6) (a) Abarca, A.; Martín, A.; Mena, M.; Yélamos, C. *Angew. Chem., Int. Ed.* **2000**, *39*, 3460–3463. (b) García-Castro, M.; Gracia, J.; Martín, A.; Mena, M.; Poblet, J.-M.; Sarasa, J. P.; Yélamos, C. *Chem.—Eur. J.* **2005**, *11*, 1030–1041. (c) Carbó, J. J.; Martínez-Espada, N.; Mena, M.; Mosquera, M. E. G.; Poblet, J.-M.; Yélamos, C. *Chem.—Eur. J.* **2009**, *15*, 11619–11631. (d) Martínez-Espada, N.; Mena, M.; Mosquera, M. E. G.; Pérez-Redondo, A.; Yélamos, C. *Organometallics* **2010**, *29*, 6732–6738.
- (7) (a) Caballo, J.; García-Castro, M.; Martín, A.; Mena, M.; Pérez-Redondo, A.; Yélamos, C. *Inorg. Chem.* **2008**, *47*, 7077–7079. (b) Caballo, J.; García-Castro, M.; Martín, A.; Mena, M.; Pérez-Redondo, A.; Yélamos, C. *Inorg. Chem.* **2011**, *50*, 6798–6808.
- (8) Herrmann, W. A.; Salzer, A. Literature, Laboratory Techniques and Common Starting Materials. In *Synthetic Methods of Organometallic and Inorganic Chemistry (Herrmann/Brauer)*; Herrmann, W. A., Ed.; Georg Thieme Verlag: New York, 1996; Vol. 1.
- (9) (a) Evans, D. F. *J. Chem. Soc.* **1959**, 2003–2005. (b) Sur, S. K. *J. Magn. Reson.* **1989**, 169–173. (c) Grant, H. D. *J. Chem. Educ.* **1995**, *72*, 39–40. (d) Bain, G. A.; Berry, J. F. *J. Chem. Educ.* **2008**, *85*, 532–536.
- (10) Farrugia, L. J. *J. Appl. Crystallogr.* **1999**, *32*, 837–838.
- (11) Sheldrick, G. M. *Acta Crystallogr., Sect. A* **2008**, *64*, 112–122.
- (12) Van der Sluis, P.; Spek, A. L. *Acta Crystallogr., Sect. A* **1990**, *46*, 194–201.
- (13) (a) *ADF 2005.01*; Department of Theoretical Chemistry, Vrije Universiteit: Amsterdam, The Netherlands. (b) Baerends, E. J.; Ellis, D. E.; Ros, P. *Chem. Phys.* **1973**, *2*, 41–51. (c) Versluis, L.; Ziegler, T. *J. Chem. Phys.* **1988**, *88*, 322–328. (d) Te Velde, G.; Baerends, E. J. *J. Comput. Phys.* **1992**, *99*, 84–98. (e) Fonseca Guerra, C.; Snijders, J. G.; Te Velde, G.; Baerends, E. J. *Theor. Chem. Acc.* **1998**, *99*, 391–403.
- (14) Vosko, S. H.; Wilk, L.; Nusair, M. *Can. J. Phys.* **1980**, *58*, 1200–1211.
- (15) (a) Becke, A. D. *J. Chem. Phys.* **1986**, *84*, 4524–4529. (b) Becke, A. D. *Phys. Rev. A* **1988**, *38*, 3098–3100.
- (16) (a) Perdew, J. P. *Phys. Rev. B* **1986**, *33*, 8822–8824. (b) Perdew, J. P. *Phys. Rev. B* **1986**, *34*, 7406–7406.
- (17) (a) Klamt, A.; Schüürmann, G. *J. Chem. Soc., Perkin Trans. 2* **1993**, 799–805. (b) Andzelm, J.; Kölmel, C.; Klamt, A. *J. Chem. Phys.* **1995**, *103*, 9312–9320. (c) Klamt, A. *J. Phys. Chem.* **1995**, *99*, 2224–2235. (d) Model implemented in the ADF package by Pye, C. C.; Ziegler, T. *Theor. Chem. Acc.* **1999**, *101*, 396–408.
- (18) López, X.; Fernández, J. A.; Romo, S.; Paul, J. F.; Kazansky, L.; Poblet, J.-M. *J. Comput. Chem.* **2004**, *25*, 1542–1549.
- (19) (a) Davies, A. G.; Luszyk, J. *J. Chem. Soc., Perkin Trans. 2* **1981**, 692–696. (b) Cummins, C. C.; Schrock, R. R.; Davis, W. M. *Organometallics* **1991**, *10*, 3781–3785. (c) Evans, W. J.; Perotti, J. M.; Kozimor, S. A.; Champagne, T. M.; Davis, B. L.; Nyce, G. W.; Fujimoto, C. H.; Clark, R. D.; Johnston, M. A.; Ziller, J. W. *Organometallics* **2005**, *24*, 3916–3931. (d) Mueller, T. J.; Ziller, J. W.; Evans, W. J. *Dalton Trans.* **2010**, *39*, 6767–6773.
- (20) Roitershtein, D.; Domingos, A.; Pereira, L. C. J.; Ascenso, J. R.; Marques, N. *Inorg. Chem.* **2003**, *42*, 7666–7673.
- (21) Li, J.-S.; Neumüller, B.; Dehnicke, K. *Z. Anorg. Allg. Chem.* **2002**, *628*, 45–50.
- (22) Varga, V.; Gyepes, R.; Pinkas, J.; Horáček, M.; Kubista, J.; Mach, K. *Inorg. Chem. Commun.* **2012**, *19*, 61–65.
- (23) Heinemann, F. W.; Gerisch, M.; Steinborn, D. *Z. Kristallogr.* **1997**, *212*, 462–464.
- (24) Czado, W.; Maurer, M.; Müller, U. *Z. Anorg. Allg. Chem.* **1998**, *624*, 1871–1876.
- (25) Carbó, J. J.; Martín, A.; Mena, M.; Pérez-Redondo, A.; Poblet, J.-M.; Yélamos, C. *Angew. Chem., Int. Ed.* **2007**, *46*, 3095–3098.
- (26) (a) Abarca, A.; Galakhov, M.; Gómez-Sal, P.; Martín, A.; Mena, M.; Poblet, J.-M.; Santamaría, C.; Sarasa, J. P. *Angew. Chem., Int. Ed.* **2000**, *39*, 534–537. (b) Aguado-Ullate, S.; Carbó, J. J.; González-del Moral, O.; Gómez-Pantoja, M.; Hernán-Gómez, A.; Martín, A.; Mena, M.; Poblet, J.-M.; Santamaría, C. *J. Organomet. Chem.* **2011**, *696*, 4011–4017.
- (27) The poor quality of crystals of **2** has precluded an accurate determination of their structure so far. However, the crystal analysis revealed structural features similar to those determined for analogous complexes $[\text{Cl}_3\text{M}\{\mu_3\text{-NH}\}_3\text{Ti}_3(\eta^5\text{-C}_5\text{Me}_5)_3(\mu_3\text{-N})\}]$ ($\text{M} = \text{Sc, Er, Lu}$) (see ref 7). Thus, crystals of **2** contain two independent molecules in the asymmetric unit but there are no substantial differences between them. Table 5 shows selected lengths for those whose coordinates have been used for the DFT calculations.
- (28) Kaim, W. *Coord. Chem. Rev.* **1987**, *76*, 187–235.